Acoustical finite-difference time-domain simulations of subwavelength geometries

John De Poorter and Dick Botteldooren

Citation: The Journal of the Acoustical Society of America **104**, 1171 (1998); doi: 10.1121/1.424325
View online: http://dx.doi.org/10.1121/1.424325
View Table of Contents: http://asa.scitation.org/toc/jas/104/3
Published by the Acoustical Society of America

Acoustical finite-difference time-domain simulations of subwavelength geometries

John De Poorter and Dick Botteldooren
Department of Information Technology, University of Gent, St. Pietersnieuwstraat 41, B-9000 Gent, Belgium

(Received 21 August 1997; accepted for publication 21 May 1998)

Accurate simulation of wave propagation around subwavelength geometries using standard finite-difference time-domain (FDTD) techniques require a fine spatial and temporal sampling resulting in high computational costs. In this paper an extension to this standard FDTD technique is proposed by means of quasi-stationary solutions on a subwavelength scale. The FDTD equations in the region near the subwavelength geometry are extended with some correction terms of which the magnitude is extracted from the quasi-stationary pressure distribution around these geometries. These pressure distributions can be calculated from the Laplace equation. Using this new technique, FDTD simulations can be based on a more coarse grid, thus reducing computational cost considerably. The accuracy of this technique is mainly determined by the accuracy of the Laplace solutions. This technique was tested with success on the simulation of resonators. It was also shown that the new FDTD equations can be extended to include viscosity effects. © *1998 Acoustical Society of America.* [S0001-4966(98)06908-2]

PACS numbers: 43.20.Bi, 43.20.Rz [DEC]

INTRODUCTION

Wave propagation can be effectively modeled using finite-difference time-domain (FDTD) simulation techniques.[1–3] This technique is based on the spatial and time discretization of the wave equation. Time-domain simulations have the advantage to allow an effective simulation of pulse responses, applicable for instance in reflectometry or scattering studies.[4,5] The simplicity of the FDTD equations, on the other hand, offers a great flexibility. The equations can be extended to non-Cartesian grids[6] and to include viscosity[7] and nonlinear effects.[8]

A limitation of all wave propagation simulation techniques is the high computational cost. For standard FDTD simulations, this cost is determined by the required fineness of the spatial discretization. A fundamental constraint concerning this discretization is that the FDTD cell size is much less (a factor of 10 to 20) than the smallest wavelength that will propagate through the investigated media. However, when special geometries smaller than this wavelength are a determining factor of the acoustical structure, the cell size has to be decreased. Some examples of possible subwavelength geometries are the mouth of a resonator determining the resonance frequency of the resonator or a rough staircase discretization of a smooth surface inducing significant errors in the results. Of course, decreasing cell size is limited by the available computer memory resources and by calculation time considerations.

Approaches to deal with this problem are presented in the literature on electromagnetics.[1] A possible way is to use the larger cell sizes based on wavelength considerations instead of those based on the smallest parts of the geometry, but to adapt the FDTD equations in cells close to the subwavelength geometry. The adaptation of the FDTD equations is based on known analytical solutions for simple geometries, e.g., thin wires or lumped circuit elements. More complex configurations are solved using expansion techniques, where the feature of interest is first simulated locally in a finer grid, and these results are exported to a more coarse grid.

In this paper, a general approach to deal with subwavelength geometries in acoustical problems is described. The pressure distribution near such geometries can be calculated using a quasi-stationary approximation of the wave equations.[9] Correction terms for the FDTD equations in the coarse grid are extracted out of this spatial distribution. The great benefit of this approach is that almost no extra calculation time and computer memory are necessary for the FDTD simulation. Only before FDTD simulations can be performed, the quasi-stationary problem has to be solved for each subwavelength geometry of interest.

Near subwavelength geometries high pressure-field gradients may occur, resulting in significant dissipative viscosity effects in the boundary layers.[10] Boundary layer theory can be introduced in a general way in the FDTD simulations.[7] Applying the quasi-stationary approximation some simplifications can be made which allow an effective simulation of the vorticity effects near the subwavelength geometries.

I. MATHEMATICAL MODEL

A. Quasi-stationary approximation of linear acoustics

The linearized Euler equation in a viscous fluid relates the acoustic velocity $\mathbf{v}$ to the acoustic pressure p,[10]

$$\rho_0 \frac{\partial \mathbf{v}}{\partial t} = -\nabla p + \mu\left[\nabla^2 \mathbf{v} + \frac{1}{3}\nabla(\nabla \cdot \mathbf{v})\right], \tag{1}$$

where ρ_0 is the equilibrium fluid density and μ is the fluid viscosity. The linearized mass conservation equation reads

$$\frac{\partial p}{\partial t} = -\rho_0 c^2 \nabla \cdot \mathbf{v}, \tag{2}$$

where c is the speed of sound in the fluid. The combination of Eq. (1) and Eq. (2) results in the viscous wave equation.[10,11]

The time evolution of both acoustical velocities and pressures can be approximated as in phase in a region much smaller than the considered wavelengths. The acoustical field inside this region will be called quasi-stationary. At each instant, this field can also be regarded as a steady flow of an incompressible fluid reducing Eq. (2) to

$$\nabla \cdot \mathbf{v} \approx 0. \tag{3}$$

Combining Eq. (1) and Eq. (3) results in

$$\nabla^2 p \approx 0, \tag{4}$$

which is the Laplace equation. Notice that this stationary-flow equation remains valid when significant viscosity effects exist in the fluid.

One can conclude that within a region which is small compared to the wavelength the instantaneous pressure can be derived from the potential equation [Eq. (4)] in combination with the boundary conditions at that moment. These boundary conditions are the pressure value or the normal derivative of the pressure field at the boundary of the examined region. Due to the linearity of the potential equation, the instantaneous pressure distribution inside the region is a linear function of the instantaneous boundary condition values.

B. FDTD formulation near subgrid geometries

For simplicity reasons, we will limit further description to a FDTD discretization in a Cartesian grid, although there are no theoretical obstacles against applying more general grids.[6] Also, we will initially ignore the viscosity effects. The FDTD equations in a staggered grid will first be derived by integrating the analytical wave equations over the Cartesian grid cells. The integral formulation of Eq. (2) over a closed cell volume V_i of which the surface S_i is divided in a set of subsurfaces $S_{i,j}$ reads

$$\frac{d}{dt}\left(\frac{1}{V_i}\int_{V_i} p \, dV\right) = -\frac{\rho_0 c^2}{V_i}\sum_j S_{i,j}\left(\frac{1}{S_{i,j}}\int_{S_{i,j}} v_n \, dS\right), \tag{5}$$

where v_n is the velocity component parallel to the outer normal vector of the surfaces $S_{i,j}$. This equation can be interpreted in terms of the mean pressure in volume V_i and the mean normal velocity components over the surfaces $S_{i,j}$, which will be the unknown physical parameters in the FDTD equations. The subsurface $S_{i,j}$ is the surface in between volume V_i and volume V_j (see Fig. 1) and is perpendicular to a coordinate axis. Adding the subsurfaces over index j results in the surface S_i enclosing the ith box with volume V_i.

A second equation describing the time derivative of the mean normal velocity components can be derived from Eq. (1) neglecting the viscosity effects,

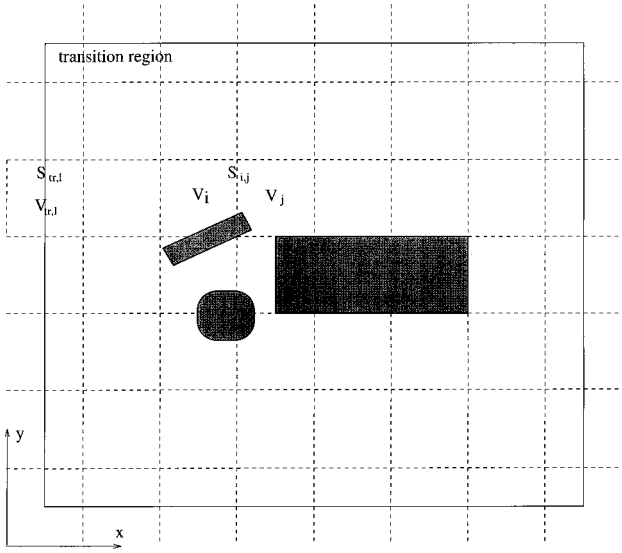

FIG. 1. Quasi-stationary region around some subwavelength geometries. The coarse Cartesian grid is insufficient to describe the geometries and the acoustical field around them. Therefore, the FDTD equations inside this region will be adapted.

$$\frac{d}{dt}\left(\frac{1}{S_{i,j}}\int_{S_{i,j}} v_n dS\right) = -\frac{1}{\rho_0}\left(\frac{1}{S_{i,j}}\int_{S_{i,j}} \frac{\partial p}{\partial n} dS\right). \tag{6}$$

To obtain a closed system of equations, the mean normal derivative of the pressure has to be estimated from the mean pressure values over the volumes V_i, which are the FDTD variables.

For a FDTD without subwavelength geometries, the mean normal derivative of the pressure of Eq. (6) is estimated by

$$\frac{1}{S_{i,j}}\int_{S_{i,j}} \frac{\partial p}{\partial n} dS = \left\langle \frac{\partial p}{\partial n} \right\rangle_{S_{i,j}} \approx \pm \frac{1}{dn_j}(\langle p \rangle_{V_j} - \langle p \rangle_{V_i}), \tag{7}$$

where dn_j is the cell size in the direction orthogonal to $S_{i,j}$, $\langle p \rangle_{V_j}$ and $\langle p \rangle_{V_i}$ are the mean pressures over the volumes V_j and V_i, respectively. The sign depends on the direction of the outer normal of $S_{i,j}$ with respect to the coordinate axes. In Eq. (7) the spatial derivative along the outer normal is approximated by the second order centered difference form. This approximation is accurate as long as third and higher order terms in dn_j of the spatial Taylor's expansion of the pressure field are negligible compared to the first and second order terms.[6] Combining Eqs. (6) and (7) and after time discretization of the resulting equation and Eq. (5) the standard FDTD equations can be obtained.[2,6] However, when subwavelength-sized structures must be modeled and the standard FDTD equations are used, one can only obtain good accuracy when the grid cell size is adapted to the dimension of these objects. This will result into a significant increase of computational costs.

Consider a subwavelength geometry with hard surfaces in a region that is discretized by a Cartesian grid (Fig. 1). The grid cell dimensions, however, are too coarse to describe the complex spatial function of the pressure field nearby this geometry or to describe the geometry itself. For this reason the right side of Eq. (7) will be a bad approximation of

$\langle \partial p/\partial n \rangle_{S_{i,j}}$. At a certain distance of the geometry, usually several times the dimensions of the geometry, Eq. (7) will again be valid. If this region around the geometry is still small compared to the smallest wavelength, a better approximation for the pressure derivative inside this region can be calculated based on the quasi-stationary approximation described in Sec. I A. We will call this region the quasi-stationary zone. The linearity of the potential problem allows us to write the instantaneous pressure field at any point inside the quasi-stationary zone as a linear function of the pressure values at the border of this zone. As is illustrated in Fig. 1, the border surface of this quasi-stationary zone can be discretized in subsurfaces, named $S_{tr,l}$. The mean pressures over these surfaces $\langle p \rangle_{S_{tr,l}}$ are the fundamental set of pressures that determine the pressures (and some derivative quantities) inside the quasi-stationary zone. This property can be applied to extend Eq. (7) for the presence of subgrid geometries resulting in

$$\left\langle \frac{\partial p}{\partial n} \right\rangle_{S_{i,j}} \approx \pm \frac{1}{dn_j} \left(\langle p \rangle_{V_j} - \langle p \rangle_{V_i} + \sum_l a_{l,S_{i,j}} \langle p \rangle_{S_{tr,l}} \right)$$

$$\approx \pm \frac{1}{dn_j} \left(\langle p \rangle_{V_j} - \langle p \rangle_{V_i} + \sum_l a_{l,S_{i,j}} \langle p \rangle_{V_{tr,l}} \right), \qquad (8)$$

where $a_{l,S_{i,j}}$ is a coefficient of the linear expression, quantifying the effect of the pressure at $S_{tr,l}$ on the correction term in surface $S_{i,j}$. In the FDTD calculation scheme, one only knows the mean pressure over volumes and not the mean pressures over surfaces. Therefore, $\langle p \rangle_{S_{tr,l}}$ is approximated by $\langle p \rangle_{V_{tr,l}}$ in Eq. (8), where $V_{tr,l}$ encloses the surface $S_{tr,l}$ (see Fig. 1). The coefficients $a_{l,S_{i,j}}$ can be calculated by solving the Laplace equation in the quasi-stationary zone with boundary conditions $\langle p \rangle_{S_l} = 1$ and $\langle p \rangle_{S_k} = 0$ for every $k \neq l$. When the quasi-stationary solutions corresponding to this boundary conditions are labelled QS,l, one can derive the correction coefficients $a_{l,S_{i,j}}$ as

$$a_{l,S_{i,j}} = \frac{\pm dn_j}{\langle p_{QS,l} \rangle_{V_{tr,l}}} \left(\left\langle \frac{\partial p_{QS,l}}{\partial n} \right\rangle_{S_{i,j}} - (\langle p_{QS,l} \rangle_{V_j} - \langle p_{QS,l} \rangle_{V_i}) \right). \qquad (9)$$

For some special cases, the Laplace equation can be solved analytically, but generally numerical techniques are necessary. Many of those calculation techniques are described in the literature.[12,13] We preferred a finite difference calculation technique because similar grids as for FDTD could be used.

Notice that in Eq. (8) the quasi-stationary assumption is only used to calculate geometrical correction terms for $\langle \partial p/\partial n \rangle_{S_{i,j}}$. Another approach is to calculate $\langle \partial p/\partial n \rangle_{S_{i,j}}$ completely out of the pressure values at the border of the quasi-stationary zone. The correction term approach, however, has the advantage that in grid cells where the correction terms are small (e.g., close to the zone borders), the wave propagation is still determined by the general FDTD algorithm instead of a quasi-stationary approximation. This improves the accuracy of the calculations.

The FDTD equations are not unconditionally stable. For a classical set of equations in a Cartesian grid the time step Δt has to fulfill following condition,

$$\Delta t < \frac{1}{c \sqrt{\frac{1}{\Delta x^2} + \frac{1}{\Delta y^2} + \frac{1}{\Delta x^2}}}, \qquad (10)$$

with Δx, Δy, and Δz the dimensions of a Cartesian grid cell in the x, y, and z direction, respectively. Because the correction terms relate the local pressures to pressures at the border of the transition zone, it can be assumed that the quasi-stationary correction terms have no effect on this condition. No exceptions to this assumption were found experimentally.

The attenuating effects of air viscosity are most significant near rigid boundaries. The existence of a velocity boundary layer decreases the mean velocity components parallel to the boundary. An analytical expression for this effect can be derived near plane boundaries in the frequency domain.[9] In time domain, this expression can be transformed to a convolution between the pressure gradient along the boundary and $t^{-1/2}$ function.[11] For practical applications, this convolution can be approximated by a recursion formula that is updated every time step.[7] In Sec. I A, it was proven that the quasi-stationary correction terms are independent of viscosity effects. Therefore, the boundary layer approach can also be applied in the velocity surfaces that are perpendicular to subwavelength rigid boundaries.

II. EVALUATION OF HELMHOLTZ RESONATORS

A. The quasi-stationary approach compared to finer grids

A Helmholtz resonator with volume V_{res}, area of the mouth surface S_{res}, and effective neck length l'_{res} has its resonance frequency f_{res} at

$$f_{\text{res}} = \frac{c}{2\pi} \sqrt{\frac{S_{\text{res}}}{V_{\text{res}} l'_{\text{res}}}}, \qquad (11)$$

with c the speed of sound (approximated for all simulations as 340 m/s). The effective neck length is higher than the physical neck length l_{res} due to the quasi-stationary flow contraction near the resonator mouth. The difference between both lengths depends on the size of the resonators mouth. For an isolated resonator with a circular mouth with radius a this difference is equal to $16a/2\pi$.[9,14]

To prove the effectiveness of the proposed quasi-stationary correction technique, resonators with physical neck length small compared to the surface of the resonator mouth are chosen. In this way the effective neck length and the resonator frequency is completely determined by flow contraction around the resonator mouth. To model these flow contractions with a classical FDTD algorithm, the FDTD cell size should be significantly smaller than the mouth dimensions. However, the simulation space will be oversampled outside the resonator mouth region because the mouth dimensions themselves are in most cases already smaller than

TABLE I. The physical characteristics (volume V_{res}, area of resonators mouth S_{res}, physical neck length l_{res}, estimated effective neck length l'_{res}, estimated resonator frequency f_{res}, area of the tube section S_{tube}) of the two investigated resonators.

Parameter	Mouth = square orifice	Mouth = circular orifice
V_{res} (m^3)	27×10^{-6}	18×10^{-6}
S_{res} (m^2)	100×10^{-6}	19.63×10^{-6}
l_{res} (m)	0	0
l'_{res} (m)	7.6×10^{-3}	4.24×10^{-3}
f_{res} (Hz)	1195	867
S_{tube} (m^2)	2500×10^{-6}	900×10^{-6}

the wavelengths considered. In this section, the results of oversampled FDTD simulations will be compared to the quasi-stationary approach.

Consider a resonator with a rectangular mouth placed on one side of a rectangular tube. The walls of the resonator and tube are considered to be acoustically hard. The characteristic dimensions of this resonator can be found in Table I. In Fig. 2(a), this resonator and tube are schematically shown in a coarse FDTD grid. Notice that the resonator mouth has the size of one grid cell surface, which is 0.01 m by 0.01 m. The effect of this resonator can be evaluated using the transmission coefficient. This coefficient is defined as the ratio of the complex pressure amplitude after the resonator at the end of the tube and the complex pressure amplitude that was injected into the tube. The frequency dependence of this coefficient characterizes the resonators effect on the zero order propagating mode of the tube. Near the resonating frequency of the resonator, the impedance of the resonator and the transmission coefficient becomes small. Away from f_{res} the resonator will have less effect on the propagating modi of the tube and the amplitude of the transmission coefficient will reach one.

The rectangular resonator tube has a length of 0.13 m. The front face and back face of the tube were modelled to have the acoustical impedance of the medium $\rho_0 c$. For plane waves this boundary conditions has the same effect as an outer radiation boundary condition.[1] At 0.015 m of the front face of the tube, a plane of transparent pressure sources parallel to this front face was placed to inject a plane wave into the tube. The transparency of the sources avoids reflection against this plane of sources. Transparent pressure sources can easily be constructed in FDTD by adding the desired time function $p_{sc}(t)$ to Eq. (5). For this application a smooth asymmetrical impulse with a relatively broad spectrum was used,

$$p_{sc}(t)=(t-t_0)e^{-(t-t_0)^2/\sigma}. \tag{12}$$

The time offset t_0 was chosen to be 5 ms and σ was 2.5×10^{-7} s^2. This pressure impulse gives rise to a plane wave impulse inside the tube with a frequency bandwidth between zero and $1/\sqrt{\sigma}$, this is 2000 Hz.

The transmission coefficient over a frequency range was calculated using the FDTD algorithm. Therefore, the signal of Eq. (12) was transmitted into the tube and the pressure response at the end of the tube was monitored during the

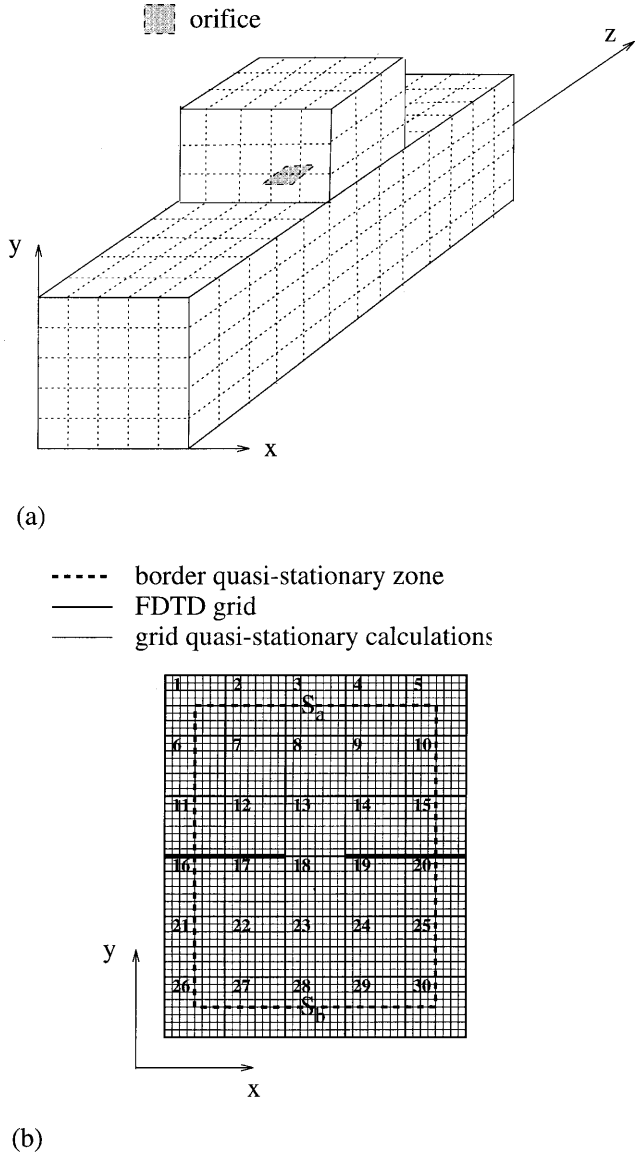

FIG. 2. (a) Scheme of a resonator inside a coarse FDTD grid. The mouth of the resonator corresponds to one FDTD cell. (b) Two-dimensional section of the grid used to calculate the quasi-stationary flow contractions around the resonator mouth.

calculations. Both time signals, the test signal, and the response are Fourier transformed and the transmission coefficient can be calculated for every frequency as the ratio of the complex signal amplitudes of response and test signal. This calculation was performed in the coarse grid and in finer FDTD grids. The finer grids had linear dimensions that were 3 times, 6 times, and 12 times smaller than the coarse FDTD grid. More details about the parameters of these calculations can be found in Table II. The time step was chosen to conform to the stability condition [see Eq. (10)]. Notice that in a first approximation the memory usage increases for each grid refinement with a third power of the one-dimensional refinement factor and the CPU time in ideal circumstances (i.e., sufficient memory resources) with the fourth power of this factor. The most accurate calculations (refinement factor = 12) are at the limit of engineering workstation possibilities as is illustrated by the figures in Table II.

The FDTD simulated transmission coefficients are

TABLE II. FDTD simulation parameters (the grid linear dimensions $\Delta x=\Delta y=\Delta z$, the time step Δt, the number of calculation steps N, number of cells that fit into the rectangular orifice n_{orifice}, memory usage, and CPU calculation time) for the simulations of the resonators with a rectangular mouth. The unit of the CPU time corresponds on a HP workstation 735/125 to 10.9 s.

Parameter	Grid 1	Grid 2	Grid 3	Grid 4
$\Delta x=\Delta y=\Delta z$ (m)	0.01	0.003 33	0.001 667	0.00083
Δt (μs)	15	5	2.5	1.25
N	2731	8192	16 384	32 768
n_{orifice}	1	9	36	144
memory usage (MBy)	0.12	1.68	12.85	102.8
CPU time (a.u.)	1	81	1296	20 736

drawn in Fig. 3. The grid refinements have a significant effect on the resonating frequency (almost a doubling). This illustrates the fact that an accurate simulation of this resonator using the classical FDTD equations requires grid dimensions of 1/340 of the wavelength corresponding to the resonating frequency. Even if the grid refinement is only limited to a region around the resonator mouth, a significant increase in the computational efforts can be expected. It is interesting to notice that the coarse grid simulations underestimate the resonating frequency. This corresponds to a overestimation of the effective neck length [see Eq. (11)] or to an overestimation of the spatial extent of the flow contraction region around the resonator mouth.

It is clear that FDTD grid refinements are not an optimal approach to this problem. The quasi-stationary solution of this problem will now be investigated. Therefore, the potential problem in the neighborhood of the resonator mouth (i.e., a rectangular orifice) will be solved in a fine grid, schematically visualized in Fig. 2(b). The simulation grid has linear dimensions which are 1/12 of the coarse grid that will be used during the FDTD simulations. Following Eq. (8), every FDTD pressure in the quasi-stationary zone border will induce a correction term for every velocity point calculation inside the quasi-stationary zone. In the two-dimensional section of Fig. 2(b), there are already 18 FDTD cells at the border of the quasi-stationary zone. However, the pressures at the border of the quasi-stationary zone around the orifice will only differ significantly before and after the orifice. At the same side of the orifice, the border pressure differences will be negligible because the border length is still small compared to the wavelength. Therefore, the number of important correction terms can be reduced to two, i.e., two correction terms for each velocity inside the quasi-stationary zone. The potential problem has only to be solved twice. For the first simulation, the pressure values at the quasi-stationary zone borders S_b before the orifice [see Fig. 2(b)] have to be put to one and pressure values at the borders S_a after the orifice to zero. For the second simulation these boundary conditions are switched. This second configuration does not have to be calculated due to the symmetry of the problem. Indeed, it can be seen that the correction term factors $a_{b,S_{i,j}}$ and $a_{a,S_{i,j}}$ are opposite. In conclusion, every pressure gradient inside the quasi-stationary zone can be written as

$$\left\langle \frac{\partial p}{\partial n} \right\rangle_{S_{i,j}} \approx \pm \frac{1}{dn_j} (\langle p \rangle_{V_j} - \langle p \rangle_{V_i} + a_{S_{i,j}} (\langle p \rangle_{S_a} - \langle p \rangle_{S_b})), \tag{13}$$

with $a_{S_{i,j}} = -a_{b,S_{i,j}} = a_{a,S_{i,j}}$. The pressures $\langle p \rangle_{S_b}$ and $\langle p \rangle_{S_a}$ can be approximated during the FDTD simulation by $\langle p \rangle_{V_3}$ and $\langle p \rangle_{V_{28}}$, respectively.

The potential problem was solved using a finite-difference calculation technique.[12] In fact our standard object-oriented FDTD software was a good template for this new software package and only some minor changes had to be implemented. An overview of the correction factors for the pressure gradients from Fig. 2(b) is given in Table III.

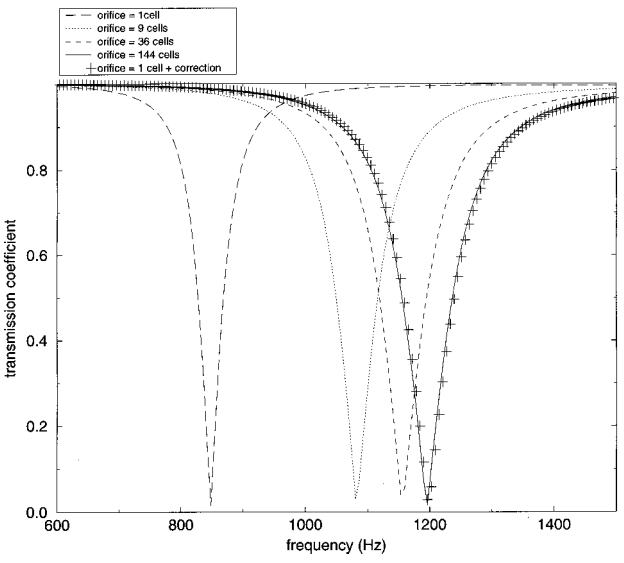

FIG. 3. Simulated frequency dependence of the transmission coefficients amplitude for the tube-resonator system. The resonator has a square resonator mouth and the effects of grid refinement is illustrated and compared to the quasi-stationary correction method.

TABLE III. Correction factors for the FDTD equations nearby a rectangular orifice with the size of an FDTD grid cell. The numbering corresponds to the notation in Fig. 2(b).

Surfaces $S_{i,j}$	Correction factor $a_{S_{i,j}}$
$S_{13,18}$	0.710
$S_{8,13}, S_{18,23}$	−0.042
$S_{12,13}, S_{18,19}$	0.157
$S_{13,14}, S_{17,18}$	−0.157
$S_{7,8}, S_{23,24}$	0.004
$S_{8,9}, S_{22,23}$	−0.004
$S_{7,12}, S_{19,24}, S_{9,14}, S_{17,22}$	−0.001

Notice that only the velocity planes closest to the orifice and inside the orifice have a significant correction factor, the others were neglected for the FDTD calculations. The transmission coefficient, simulated with the new FDTD equations, is also printed in Fig. 3. There is a very good agreement with the results obtained using a refinement factor of 12. The quasi-stationary calculations were performed in a grid that was as fine. A similar agreement was found between the FDTD calculations performed in the grids with the other refinement factors (3 and 6) and the FDTD calculations in the coarse grid but using correction coefficients of quasi-stationary calculations in corresponding grids. These facts suggest that the error introduced by using a quasi-stationary approach can be neglected. We can therefore conclude that the accuracy of the FDTD simulations using quasi-stationary solutions is only determined by the accuracy of the quasi-stationary solution itself.

The phase variations of the transmission coefficient were also examined. The phase results in the fine grid were compared to the phase results in a coarse grid with corrected FDTD equations. The maximum phase error is around 2.9 degrees and is located near the phase jump at the resonance frequency. Taking into account the spatial sampling of the problem in the coarse grid, it can be shown that these phase errors are not related to grid dispersion.[2] Therefore, these phase errors are related to the quasi-stationary methodology but they are not significant for most FDTD applications.

The CPU time and computer memory of the FDTD simulations were not significantly increased by the few correction terms. Thus the FDTD simulation is done with the computer costs corresponding to the coarse grid, but with an accuracy corresponding to the accuracy of the quasi-stationary simulations. Any other FDTD simulation including square orifices with dimensions of one grid cell can be simulated using the same correction factors and with the same low computational costs.

B. The quasi-stationary approach compared to analytical approximations

In this section we will demonstrate the potentials of the technique for the simulation of subgrid cell structures. Therefore, a resonator with a circular mouth will be examined. An advantage of this circular structure is that analytical approximations can be found describing the resonator impedance.[14]

A resonator configuration was studied similar to the one in Fig. 2(a). The spatial dimensions of resonator and tube can be found in Table I. The resonator mouth consisted of a circular orifice with a diameter that is equal to 0.005 m. The FDTD simulation was performed in a coarse Cartesian grid with $\Delta x=\Delta y=\Delta z=0.01$ m. In advance, the quasi-stationary correction terms were calculated in two finer grids with cell sizes of 0.001 m (grid 1) and 0.0005 m (grid 2), corresponding to one fifth and one tenth of the orifice diameter, respectively. The discretization of the circular orifice in these grids can be seen in Fig. 4. The most significant correction term $S_{13,18}$ was obtained from the quasi-stationary calculations in grid 1 and grid 2, resulting in -0.310 and -0.359, respectively. Notice that these correction factors are for one part determined by the field contractions around the orifice, but for another part by the fact that the pressure gradient is by definition zero for 80% of surface $S_{13,18}$.

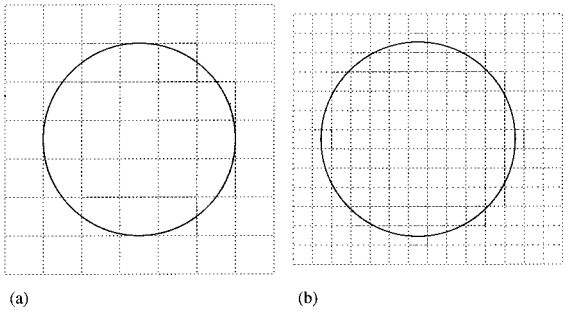

FIG. 4. Discretization of a circular orifice with a diameter equal to 0.005 m in a Cartesian grid with cell sizes of 0.001 m (a) and 0.0005 m (b).

The transmission coefficient obtained using the quasi-stationary based FDTD simulations in the coarse grid are compared to analytical results in Fig. 5. The resonance frequency differs by 2% for the calculation using the correction factor of grid 1 and by 0.7% for the correction factor based on grid 2. These results prove that an accurate simulation of the subwavelength circular orifice is possible using the quasi-stationary correction method. The computer resources used are minimal once the necessary correction coefficients are determined.

C. Combination with viscosity effects

In experimental practice, acoustic energy absorption in the resonator exists mainly as a consequence of viscosity effects.[9,14] To illustrate that these effects can also be introduced in this quasi-stationary concept, we included viscosity effects in the circular resonator on the basis of a boundary layer formulation. The viscous attenuation will only be important near significant pressure gradients, that is, at the resonator mouth. Therefore, only the FDTD equation in the circular orifice will be compensated for viscosity effects. The

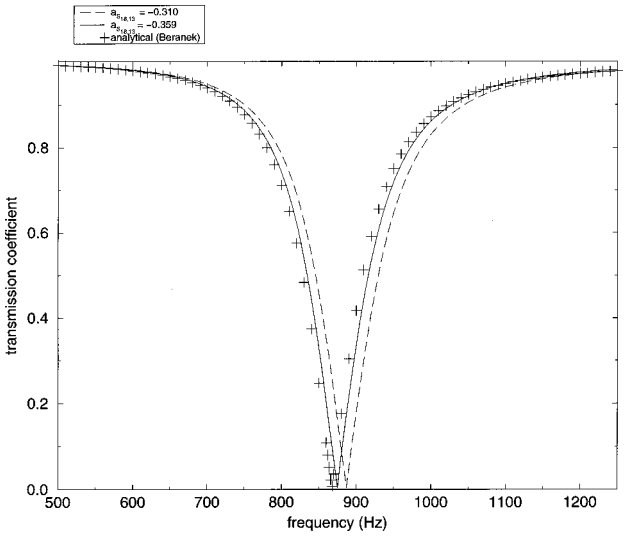

FIG. 5. Simulated frequency dependence of the transmission coefficients amplitude for the tube-resonator system with a circular orifice. The FDTD simulations based on the quasi-stationary correction terms are compared to the analytical result (Ref. 14).

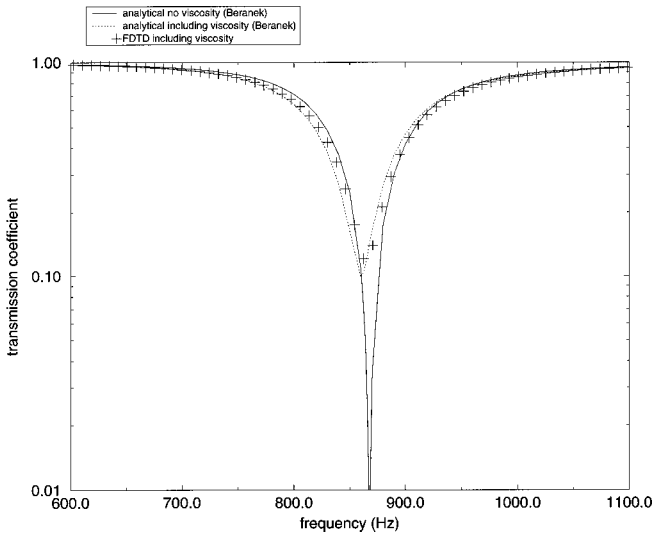

FIG. 6. Frequency dependence of the transmission coefficients amplitude for the tube-resonator system with a circular orifice including viscosity effects. The FDTD simulation is compared to the analytical results (Ref. 14).

viscous correction term [of Eq. (1)] is calculated using the results for viscous flow near an infinite plate.[7]

The effect on the transmission coefficient based on FDTD simulations is compared in Fig. 6 to the analytical expression that is also based on the viscous flow near an infinite-plate.[14] The good agreement between analytical and FDTD calculations proves that vorticity can be effectively simulated using FDTD. We must remark here that the infinite-plate boundary layer solution underestimates the viscosity effects in resonators necks that are short compared to the boundary layer thickness.[15,16] The viscous absorption will therefore be higher when the described resonator with very short physical neck length should be tested experimentally. However, it was not the goal of this paper to introduce a better estimation than the infinite-plate boundary layer solution. We only wanted to illustrate the possibility to combine viscosity effects with the subwavelength FDTD formalism. Viscous effects and the reliability of the used simplifications for more general configurations are now being examined in greater detail.

III. CONCLUSIONS

The extension of the FDTD equations with correction terms in a region around subwavelength structures allows for efficient calculation of wave propagation around such structures. Once the necessary correction terms are calculated for a specific geometry, this geometry can be included in FDTD simulations without any additional computational cost. It is considered in the FDTD equations as a subgrid object.

It was shown that the accuracy of this technique was determined by the accuracy of the correction factors, which is in turn determined by the accuracy of the Laplace solutions. The principle of using quasi-stationary solutions does not introduce significant additional error. Also, it was shown that for a specific configuration this quasi-stationary FDTD technique can be extended to include viscosity effects.

[1] K. Kunz and R. Luebbers, in *The Finite Difference Time Domain Method for Electromagnetics* (CRC, Boca Raton, 1993).
[2] D. Botteldooren, ''FDTD-simulation of low frequency room acoustic problems,'' J. Acoust. Soc. Am. **98**, 3302–3308 (1995).
[3] J. LoVetri, D. Mardare, and G. Soulodre, ''Modeling of the seat dip effect using finite-difference time-domain method,'' J. Acoust. Soc. Am. **100**, 2204–2212 (1996).
[4] R. Stephen, ''Modeling sea surface scattering by the time-domain finite-difference method,'' J. Acoust. Soc. Am. **100**, 2070–2078 (1996).
[5] M. Veysoglu and C. Cooke, ''Acoustic time-domain reflectometry for irregular surface recognition,'' J. Acoust. Soc. Am. **99**, 444–454 (1996).
[6] D. Botteldooren, ''Acoustical finite-difference time-domain simulation in a quasi-Cartesian grid,'' J. Acoust. Soc. Am. **95**, 2313–2319 (1995).
[7] D. Botteldooren, ''Vorticity and entropy boundary conditions for acoustical finite-difference time-domain simulations,'' J. Acoust. Soc. Am. **102**, 170–178 (1997).
[8] D. Botteldooren, ''Numerical model for moderately nonlinear sound propagation in three-dimensional structures,'' J. Acoust. Soc. Am. **100**, 1357–1367 (1996).
[9] L. Cremer and H. A. Müller, in *Principles and Applications of Room Acoustics* (Applied Science, London, 1978), Vol. 2.
[10] A. Pierce, in *Acoustics, An Introduction to Its Physical Principles and Applications* (McGraw-Hill, New York, 1981).
[11] T. L. Szabo, ''Time domain wave equations for lossy media obeying a frequency power law,'' J. Acoust. Soc. Am. **96**, 491–500 (1994).
[12] A. Mitchell and D. Griffiths, in *The Finite Difference Method in Partial Differential Equations* (Wiley, New York, 1990).
[13] C. Brebbia, J. Silva, and P. Partidge, in *Boundary Element Methods in Acoustics, Computational Formulation*, edited by R. Ciskowski and C. Brebbia (Computational Mechanics, Southampton, 1991).
[14] L. Beranek and I. Vér, in *Noise and Vibration Control Engineering* (Wiley, New York, 1992).
[15] U. Ingard, ''On the theory and design of acoustic resonators,'' J. Acoust. Soc. Am. **25**, 1037–1061 (1953).
[16] A. Kuckes and U. Ingard, ''A note on acoustic boundary dissipation due to viscosity,'' J. Acoust. Soc. Am. **25**, 798–799 (1953).